Regioisomeric Spirobifluorene CANAL Ladder Polymers and Their Gas Separation Performance

Ashley M. Robinson, Yan Xia*

Department of Chemistry, Stanford University, Stanford, California 94305, United States.

ABSTRACT: We synthesized and characterized two isomeric microporous hydrocarbon ladder polymers from catalytic arene norbornene annulation (CANAL) of regioisomeric bis-norbornene fused spirobifluorenes, where the ladder chains are connected either through the same fluorene unit or across two different fluorene units in spirobifluorene. This pair of isomeric polymers were used to investigate the effect of ladder macromolecular structures on the microporosity and transport properties. Both polymers form mechanically intact films with thermal stability up to 480 °C and relatively high BET surface areas. The polymer formed from 2,7-dibromospirobifluorene showed higher BET surface areas and higher gas permeability than the polymer from 2,2'-dibromospirobifluorene despite similar intersegmental spacing as indicated by X-ray scattering. The aging behavior for both polymers followed the same trend as the previously reported CANAL-fluorene polymers, with dramatically increased permselectivities over time resulting in gas separation performance above the 2008 upper bounds for H_2/CH_4 and O_2/N_2.

In the past decade, polymers of intrinsic microporosity (PIMs) have garnered widespread interest as potential next generation materials for energy-efficient membrane-based gas separations, defining the new performance upper bounds for polymer membranes.[1-8] PIMs predominantly consist of two types of rigid and contorted ladder-type backbone structures with ladder aryl ether (aka PIM-1 type) or Tröger's Base (TB) linkages. The structural rigidity and contortion lead to frustrated chain packing in the solid state, resulting in abundant microporosity and exceptionally high gas permeabilities. Extensive research has been devoted to varying the PIM backbone motifs by including ethanoanthracene, spirobisindane, spirobifluorene, triptycene, and other iptycene structures.[3, 9-13] Despite the large number of PIM examples and their applications in membrane gas separations, very limited understanding still exists on how the PIM backbone structures affect the gas transport properties of the resulting membranes. The actual contorted PIM structures are typically more complex than their nominally drawn structures, and as the backbone motif is changed, additional molecular parameters such as the distribution of topologies, chain packing, and segmental rigidity will vary. For example, the TB linkage is chiral and different regioisomers may also be found in TB formation, so the actual TB-PIMs may contain more complex repeat unit structures than the nominally drawn structures.

Early investigation on polyimides (PIs) prepared from *para*- and *meta*- aromatic diamines, such as 3,3'- and 4,4'-diaminodiphenylsulfones or 3,3'- and 4,4'- oxydianilines (**Figure S1A**), revealed higher permeability and lower permselectivity in *para*-connected PIs, which has been attributed to variations in gas diffusion through the polymer films.[14-16] According to the Brandt model, small molecule diffusion through a polymer occurs through thermally activated motions of small polymer chain segments that form transient gaps between free volume elements (FVEs).[14, 17] Less efficient chain packing and more rotational mobility of the phenyl group in *para*-connected PIs led to reduction of the activation energy of diffusion, resulting in increased gas permeability and decreased permselectivity.[14-16] More recently, comparing two microporous PIs from diamino-triptycene regioisomers, Ma and coworkers showed that PIs synthesized from 2,7-diamino-triptycene exhibited lower permeability and higher permselectivity than PIs from 2,6-diaminotriptycene (**Figure S1B**), and this observation in different transport properties was attributed to tighter chain packing in PIs from 2,7-diamino-triptycene as suggested by X-ray diffraction.[18] This difference in chain packing was further attributed to the larger dipole moment calculated for 2,7-diamino-triptycene (2.47 vs. 1.83 Debye).[18]

Investigations on how similar or isomeric structures in PIMs may affect their gas transport properties are emerging. McKeown and coworkers compared the spirobifluorene structural unit with spirobisindane and attributed the observed higher permselectivity for PIMs consisting of spirobifluorene to the enhanced rigidity of its spirocyclic linkage over spirobisindane.[3] More recently, McKeown also investigated the effect of incorporating a series of triptycene-like structures in TB-PIMs, specifically PIM-EA-TB, PIM-Trip-TB, and PIM-BTrip-TB (**Figure S1C**). The polymers containing bulkier triptycene structures resulted in higher permeability because of increased interchain distances between the larger structural units.[10, 12] Ma and coworkers used pure 2,6 and 2,7-diaminotriptycene regioisomers to synthesize TB-PIMs (**Figure S1B**). TB-PIMs prepared using either pure isomer exhibited higher selectivity than those synthesized from the regioisomeric mixture (e.g., H_2/CH_4 selectivity of 34.9 and 35.7 for the polymers from 2,6 and 2,7-diaminotriptycene

Scheme 1. Synthesis of Two CANAL-SBF Isomeric Ladder Polymers

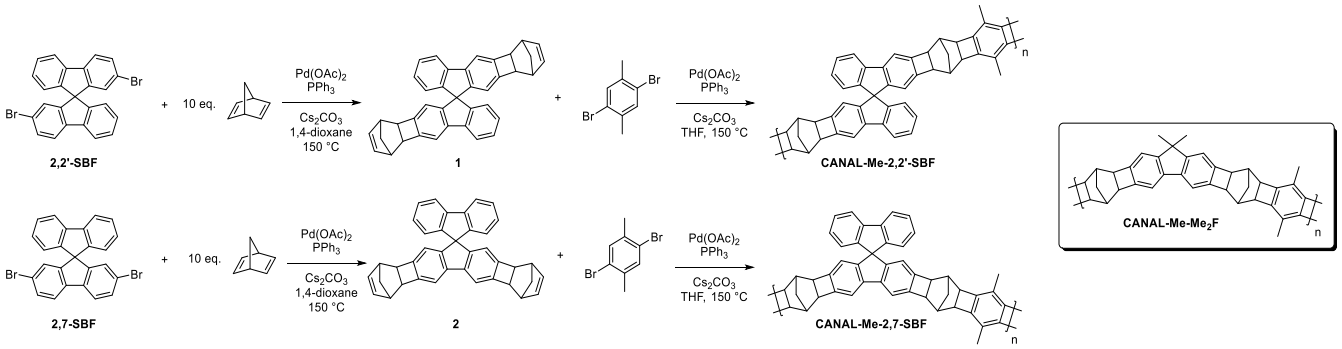

respectively instead of 25.0 for those from the regioisomeric mixture) and higher activation energy of permeation (0.0575 or 0.0740 kcal/mol for the polymers from 2,6 and 2,7-diaminotriptycene respectively instead of 0.0404 kcal/mol for those from the regioisomeric mixture).[19] The authors claimed that this interesting difference is due to the tighter and more uniform chain packing of PIMs from pure regioisomers. Hu *et al.* examined TB polymers synthesized from norbornyl bis-benzocyclobutene motifs containing *syn* or *anti* diamines (**Figure S1D**).[20] Regioisomeric formation of TB was avoided by placing the amino group *ortho* to a methyl group, limiting the TB formation to only one available reaction site. While negligible differences were observed in micropore size distributions measured by BET N_2 adsorption analysis between the PIMs synthesized from pure regioisomeric diamines, the PIMs from *syn* isomer gave slightly higher selectivity than those from the *anti* isomer.

We have developed a new type of microporous ladder polymers via catalytic arene-norbornene annulation (CANAL), using dibromoarenes and norbornadiene as the building blocks.[21-24] The resulting CANAL ladder polymers have rigid and frequently contorted hydrocarbon backbones, resulting in abundant ultra-microporosity (<7 Å), and exhibit excellent thermal stability with no detectable glass transition before their thermal decomposition temperatures. We also recently showed that CANAL polymers with three-dimensionally contorted structures exhibit unusual aging behavior and superior gas transport properties.[25] In particular, CANAL polymers consisting of ladder-type norbornyl-fused fluorene or dihydrophenanthrene repeat units exhibited an unprecedented combination of high selectivities and permeabilities upon aging.[25]

Encouraged by the promising membrane performance, we are interested in understanding the effects of structural variations in CANAL polymers on gas transport properties. We sought to use dibromoarene isomers as the constituent monomers in the ladder polymer synthesis to examine how subtle variations in molecular structures and chain geometry impact the polymer properties. Herein, we report the synthesis and study of a pair of isomeric CANAL ladder polymers containing spirobifluorene (SBF) repeat units, where the ladder chains are connected either through the same fluorene unit or across two different fluorene units in SBF (**Scheme 1**). The difference in the chain connectivity is expected to impact the chain configuration and the degree of ladder chain contortion. Even though the SBF motif has been used in PIM synthesis, this pair of SBF isomeric linkages have not been investigated. The predominant PIM-1 type PIMs require spirocyclic contortion in their backbones to provide solubility, and thus do not allow the comparison of SBF isomeric linkages. On the other hand, both CANAL-SBF isomeric polymers we have synthesized are soluble, allowing comparison of their gas transport properties alongside our previously reported fluorene-based CANAL polymer, CANAL-Me-Me_2F (Scheme 1),[25] to further elucidate the necessary features in these polymers that lead to their high separation performance after aging.

Table 1. Properties of CANAL Ladder Polymers

Polymer	M_n (kDa)	Đ	T_d, 5% (°C)	Char Yield (%)	S_{BET} (m^2/g)
CANAL-Me-Me_2F	48	2.06	487	83.7%	1156
CANAL-Me-2,2'-SBF	21	2.53	499	84.8%	508
CANAL-Me-2,7-SBF	25	3.08	487	86.6%	691

We synthesized two isomeric CANAL-SBF polymers using our previously reported two-step protocol (**Scheme 1**). First, 2,2'- or 2,7-dibromo SBF was reacted with excess norbornadiene in the presence of a palladium catalyst to give dinorbornenes **1** and **2** in 60% yield. CANAL polymerization of the dinorbornenes with 2,5-dibromo-*p*-xylene formed CANAL-Me-2,7-SBF and CANAL-Me-2,2'-SBF with modest molecular weights (**Table 1, Figure S2**). ^{1}H NMR spectroscopy of **1** and **2** as well as the isolated polymers showed the presence of all the expected signals from the CANAL ladder linkages, including the characteristic benzylic signal from the benzocyclobutene linkage around 3.1 ppm (**Figures S3-S8**). Signals corresponding to all aromatic protons in the SBF units were also observed at the expected integration of intensity. Both CANAL–SBF polymers exhibited remarkably high thermal stability with the onset of thermal decomposition at 5% mass loss (T_d, 5%) around 490 °C (**Figure S9**) and high carbonization yields of 85% at 800 °C. No signals suggesting a glass transition were observed for either polymer by differential scanning

calorimetry up to their thermal decomposition temperature (**Figure S9**).

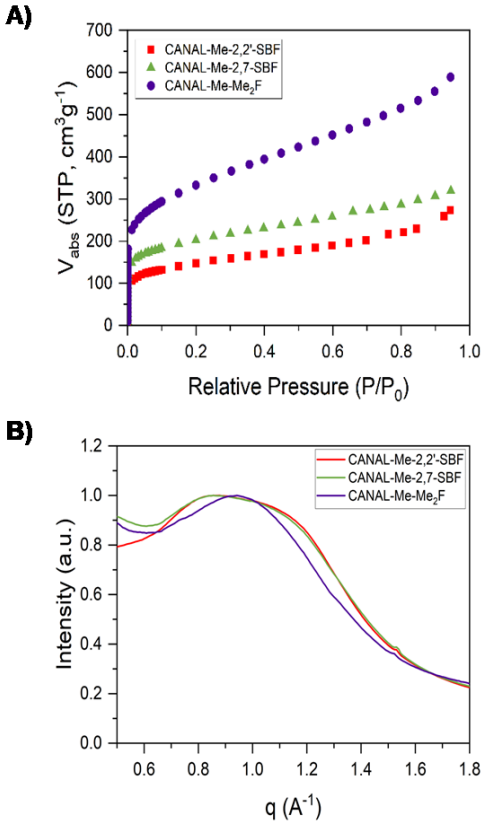

Figure 1. A) Nitrogen sorption isotherms of CANAL polymer powders at 77K and B) X-ray scattering of CANAL polymer films; CANAL-Me-2,2'-SBF, CANAL-Me-2,7-SBF, and CANAL-Me-Me_2F.

We investigated the BET surface areas and microporosity of the CANAL-SBF polymer powders using cryogenic nitrogen sorption up to 1 bar. Both polymers exhibited Type II isotherms with significant microporosity (**Figure 1A**). Moderate BET surface areas of 508 and 691 m^2g^{-1} were calculated for CANAL-Me-2,2'-SBF and CANAL-Me-2,7-SBF respectively. The lower BET surface area for CANAL-Me-2,2'-SBF may suggest less accessible free volume or more compact chain configuration and/or packing arising from frequent spirocyclic right angles through the ladder backbone. CANAL-Me-2,7-SBF can be viewed as a derivative of CANAL-Me-Me_2F containing bulkier fluorene substituents. Interestingly, CANAL-Me-2,7-SBF exhibited reduced BET surface area compared to CANAL-Me-Me_2F (691 instead of 1156 m^2g^{-1}), suggesting that the bulkier fluorene substituents occupy rather than create additional free volume.

Wide angle X-ray scattering of both CANAL-SBF polymers (**Figure 1B**) displayed a broad amorphous halo, typically observed for PIMs, owing to the contrast between voids and polymer chains. Both polymers exhibited nearly identical scattering signals with maximum intensity ranging from 5.7 to 7.4 Å, which are broader than that of CANAL-Me-Me_2F, suggesting a wider range of chain-chain distances in their packing. However, X-ray scattering does not provide information on the connectivity between FVEs.

Both polymers were soluble in chloroform and formed intact but brittle films (approximately 120 µm thick) via slow evaporation of their chloroform solutions. The much less robust films from these two polymers compared to CANAL-Me-Me_2F may be attributed to their lower molecular weights and lower solubility. The films were then heated in vacuum at 120 °C for 24 h to remove residual casting solvent. Pure-gas permeation experiments were performed using H_2, CH_4, N_2, O_2, and CO_2 on three separate films for each polymer to verify the results (**Table 2, Figure S10**).

Films of CANAL-Me-2,2'-SBF showed lower permeability than CANAL-Me-2,7-SBF for all gases. Freshly prepared films of CANAL-Me-2,2'-SBF and CANAL-Me-2,7-SBF exhibited H_2 permeability of 1200 and 3300 barrer and CO_2 permeability of 1370 and 5200 barrer respectively. CANAL-Me-2,2'-SBF demonstrated slightly higher permselectivity than CANAL-Me-2,7-SBF, with H_2/CH_4 selectivity of 9 vs. 5 and CO_2/CH_4 selectivity of 10 vs. 7.8 respectively. We attributed this difference in gas permeability to the reduced accessible free volume of CANAL-Me-2,2'-SBF.

As previously observed with other CANAL-fluorene polymers,[25] both CANAL-SBF polymers displayed substantial improvement in performance as they aged. Physical aging is a commonly observed process for PIMs, where excess free volume in the polymer film is reduced as polymer chains densify over time towards their equilibrium packing state.[26-28] Traditionally, aging of PIMs leads to decreased permeability and increased selectivity that approximately follows the upper bound trade-off relationships.[7, 28] Similar to the aging behavior that was observed for CANAL-fluorene polymers, CANAL-SBF polymers exhibited pronounced increases in selectivity during physical aging with only modest drops in permeability for H_2, CO_2, and O_2, leading to performance above the 2008 upper bounds for H_2/CH_4, and O_2/N_2 (**Figure 2, Table 2**). After physical aging, the order of gas permeabilities changed for both polymers, with PH_2 becoming larger than PCO_2. CANAL-Me-2,2'-SBF and CANAL-Me-2,7-SBF aged for 170 days exhibited H_2 permeability of 1140 and 2400 barrer and CO_2 permeability of 640 and 1400 barrer respectively. This trend suggests an aging mechanism that increases size-selectivity through a molecular sieving effect. Both CANAL-SBF polymers showed a greater decrease in permeability for larger gases after aging 170 days. CANAL-Me-2,2'-SBF exhibited 22%, 52%, and 80% decrease in permeability for H_2, CO_2, and CH_4 respectively. CANAL-Me-2,7-SBF exhibited 27%, 73%, and 92% decrease in permeability for H_2, CO_2, and CH_4 respectively. As a result, after aging CANAL-Me-2,2'-SBF and CANAL-Me-2,7-SBF demonstrated H_2/CH_4 selectivity of 42 and 44 and CO_2/CH_4 selectivity of 23 and 26 respectively. Both CANAL-SBF polymers displayed the same selective aging trend despite differences in gas permeability, providing further evidence that the observed high selectivity is due to the formation of diffusion-controlled bottlenecks between FVEs upon aging rather than the average size of FVEs.

CANAL-SBF polymers were compared with the previously reported CANAL-Me-Me_2F polymer after similar processing conditions (120 μm films heated in vacuum at 120 °C for 24 h). While the polymers all displayed the same aging trend, CANAL-Me-Me_2F demonstrated the highest permeabilities both before and after aging (**Figure 2, Table 2**). The bulkier SBF group did not lead to increased microporosity or permeability.

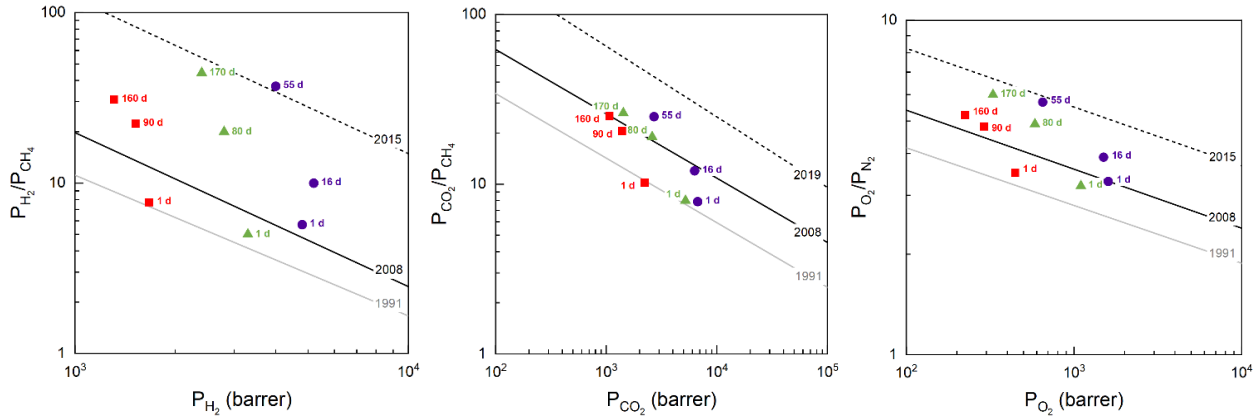

Figure 2. Pure-gas permeation properties of CANAL-Me-2,2′-SBF (red squares), CANAL-Me-2,7-SBF (green triangles), and CANAL-Me-Me_2F (purple circles) relative to the 1991 and 2008 upper bounds.[2, 29] Additional upper bounds proposed in 2015 or 2019 are shown with dashed lines.[6, 8]

Table 2. Gas Permeabilities and Ideal Permselectivities of CANAL Ladder Polymers

Polymer (Aging time in days)	Permeability (barrer)					Ideal Permselectivity			
	H_2	N_2	O_2	CH_4	CO_2	H_2/N_2	H_2/CH_4	O_2/N_2	CO_2/CH_4
CANAL-Me-2,2′-SBF (1)	1670 ±60	126 ±5	450 ±20	218 ±8	2230 ±80	13	7.7	3.5	10
CANAL-Me-2,2′-SBF (90)	1500 ±50	60 ±2	290 ±10	68 ±2	1390 ±50	25	22	4.8	21
CANAL-Me-2,2′-SBF (160)	1300 ±50	43 ±2	225 ±9	43 ±2	1070 ±40	30	31	5.2	25
CANAL-Me-2,7-SBF (1)	3300 ±200	350 ±20	1100 ±60	660 ±40	5200 ±300	9.5	5.0	3.2	7.8
CANAL-Me-2,7-SBF (80)	2800 ±100	119 ±5	590 ±20	139 ±5	2600 ±100	24	20.2	4.9	19
CANAL-Me-2,7-SBF (170)	2400 ±100	55 ±2	330 ±10	54 ±2	1400 ±60	44	44	6.0	26
CANAL-Me-Me_2F (1)[a]	4800 ±200	500 ±20	1600 ±60	840 ±30	6700 ±200	9.6	5.7	3.3	7.9
CANAL-Me-Me_2F (16)[a]	5200 ±200	380 ±10	1500 ±50	510 ±20	6300 ±200	14	10	3.9	12
CANAL-Me-Me_2F (55)[a]	4000 ±100	114 ±4	650 ±20	109 ±4	2700 ±90	35	37	5.7	25

[a] Data from ref. (25).

Instead, the similar backbone structures of CANAL-Me-2,7-SBF and CANAL-Me-Me_2F led to comparable aging trends but introducing the spirocyclic SBF linkages to CANAL polymers resulted in notably reduced permeability.

We used the time-lag method to determine diffusion (*D*) and solubility (*S*) coefficients for fresh and aged CANAL films based on the solution diffusion model (*P* = *DS*). **Table 3** displays diffusion coefficients for N_2, O_2, CH_4, and CO_2 as well as the diffusion and solubility selectivities for CO_2/CH_4 and O_2/N_2 for each film at different aging times.

Table 3. Diffusion coefficients of gases in CANAL ladder polymer films and their CO_2/CH_4 and O_2/N_2 diffusion and solubility selectivities

Polymer (aging time in days)	D (x10^8 cm^2 s^{-1})				α (CO_2/CH_4)		α (O_2/N_2)	
	N_2	O_2	CH_4	CO_2	α_D[b]	α_S[c]	α_D[b]	α_S[c]
CANAL-Me-2,2'-SBF (1)	45.6	141	17.9	90.8	5.07	2.02	3.09	1.14
CANAL-Me-2,2'-SBF (90)	20.3	87.3	5.22	50.6	9.69	2.11	4.30	1.14
CANAL-Me-2,2'-SBF (160)	15.2	79.4	3.69	37.2	10.1	2.51	5.22	1.00
CANAL-Me-2,7-SBF (1)	125	352	53.8	254	4.72	1.66	2.82	1.13
CANAL-Me-2,7-SBF (80)	40.6	168	11.7	126	10.8	1.75	4.13	1.18
CANAL-Me-2,7-SBF (170)	16.2	82.7	3.75	45.8	12.2	2.16	5.10	1.20
CANAL-Me-Me_2F (1)[a]	140	410	62	310	5.00	1.96	2.93	1.11
CANAL-Me-Me_2F (16)[a]	91	350	31.8	260	8.18	1.90	3.85	1.00
CANAL-Me-Me_2F (55)[a]	27	150	6.8	80	11.8	2.15	5.56	1.00

[a] Data from ref. (25). [b] Diffusion selectivity. [c] Solubility selectivity.

Physical aging led to a considerable decrease in diffusion coefficients paired with a large increase in diffusion selectivity for CO_2/CH_4 and O_2/N_2 for both CANAL-SBF polymers. Meanwhile, solubility selectivity was relatively unaffected by physical aging. These results suggest that both CANAL-SBF polymers follow the same aging mechanism as other CANAL fluorene polymers. In the putative aging mechanism, bottlenecks between FVEs become narrower as the films age, restricting the transport of larger gases (such as N_2 and CH_4) without significantly impacting the transport of smaller gases (such as H_2, CO_2, and O_2).[25]

In summary, we synthesized two isomeric microporous ladder polymers, CANAL-Me-2,7-SBF and CANAL-Me-2,2'-SBF, from regioisomeric dibromospirobifluorenes. The polymers were characterized by NMR spectroscopy, thermal analysis, nitrogen sorption isotherms, WAXS, and single gas permeation experiments. CANAL-Me-2,2'-SBF with a spirocyclic linkage through the backbone in each repeat unit gave lower BET surface area and gas permeability, which we attributed to reduced accessible free volume. Despite this key difference in structure and permeability, both polymers exhibited the selective aging trend observed for our previously reported CANAL-fluorene polymers. Diffusivity coefficients, calculated using time-lag permeability measurements, indicated that the physical aging process is diffusivity controlled. After 170 days of aging, the gas separation performance of these polymers is above the 2008 upper bounds for H_2/CH_4 and O_2/N_2. Overall, the aging behavior of both CANAL-SBF polymers is qualitatively similar to that of CANAL-Me-Me_2F, despite their lower permeability.

ASSOCIATED CONTENT

Supporting Information. Experimental procedures, GPC traces, TGA/DSC traces, permeability measurements, and NMR spectra. This material is available free of charge via the Internet at http://pubs.acs.org.

AUTHOR INFORMATION

Corresponding Author

* Email: yanx@stanford.edu

Author Contributions

The manuscript was written through contributions of all authors.

Funding Sources

This research was supported by DOE (DE-SC0023252) and the Stanford Hydrogen Initiative.

Notes

The authors declare no competing financial interests.

ACKNOWLEDGMENT

This material is based upon work supported by the U.S. Department of Energy, Office of Science, Separation Science, under Award Number DE-SC-0023252. We thank Jing Ying Yeo for N_2 sorption measurements, Dr. Yue Jiang for TGA/DSC measurements, and Yunfei Wang and Dr. Chenhui Zhu for WAXS measurements using beamline 7.3.3 of the Advanced Light Source, which is a DOE Office of Science User Facility under contract no. DE-AC02-05CH11231.

REFERENCES

(1) Budd, P. M.; Elabas, E. S.; Ghanem, B. S.; Makhseed, S.; McKeown, N. B.; Msayib, K. J.; Tattershall, C. E.; Wang, D. Solution-Processed, Organophilic Membrane Derived from a Polymer of Intrinsic Microporosity. *Adv. Mater.* **2004**, *16* (5), 456-459.

(2) Robeson, L. M. The upper bound revisited. J. Membr. Sci. **2008**, *320* (1), 390-400.

(3) Bezzu, C. G.; Carta, M.; Tonkins, A.; Jansen, J. C.; Bernardo, P.; Bazzarelli, F.; McKeown, N. B. A Spirobifluorene-Based Polymer of Intrinsic Microporosity with Improved Performance for Gas Separation. *Adv. Mater.* **2012**, *24* (44), 5930-5933.

(4) Carta, M.; Malpass-Evans, R.; Croad, M.; Rogan, Y.; Jansen, J. C.; Bernardo, P.; Bazzarelli, F.; McKeown, N. B. An Efficient Polymer Molecular Sieve for Membrane Gas Separations. *Science* **2013**, *339* (6117), 303-307.
(5) Ghanem, B. S.; Swaidan, R.; Ma, X.; Litwiller, E.; Pinnau, I. Energy-Efficient Hydrogen Separation by AB-Type Ladder-Polymer Molecular Sieves. *Adv. Mater.* **2014**, *26* (39), 6696-6700.
(6) Swaidan, R.; Ghanem, B.; Pinnau, I. Fine-tuned intrinsically ultramicroporous polymers redefine the permeability/selectivity upper bounds of membrane-based air and hydrogen separations. ACS Macro Lett. **2015**, *4* (9), 947-951.
(7) Low, Z.-X.; Budd, P. M.; McKeown, N. B.; Patterson, D. A. Gas permeation properties, physical aging, and its mitigation in high free volume glassy polymers. *Chem. Rev.* **2018**, *118* (12), 5871-5911.
(8) Comesaña-Gándara, B.; Chen, J.; Bezzu, C. G.; Carta, M.; Rose, I.; Ferrari, M.-C.; Esposito, E.; Fuoco, A.; Jansen, J. C.; McKeown, N. B. Redefining the Robeson Upper Bounds for CO_2/CH_4 and CO_2/N_2 Separations Using a Series of Ultrapermeable Benzotriptycene-Based Polymers of Intrinsic Microporosity. Energy Environ. Sci. **2019**, *12*, 2733-2740.
(9) Park, J.; Yoon, H. W.; Nassr, M.; Hill, M. R.; Paul, D. R.; Freeman, B. D. Pure- and mixed-gas transport properties of a microporous Troger's Base polymer (PIM-EA-TB). *Polymer* **2021**, *236*, 124295.
(10) Carta, M.; Croad, M.; Malpass-Evans, R.; Jansen, J. C.; Bernardo, P.; Clarizia, G.; Friess, K.; Lanc, M.; McKeown, N. B. Triptycene Induced Enhancement of Membrane Gas Selectivity for Microporous Troger's Base Polymers. *Adv. Mater.* **2014**, *26* (21), 3526-3531.
(11) Corrado, T. J.; Huang, Z. H.; Huang, D. Z.; Wamble, N.; Luo, T. F.; Guo, R. L. Pentiptycene-based ladder polymers with configurational free volume for enhanced gas separation performance and physical aging resistance. *PNAS* **2021**, *118* (37), 7.
(12) Rose, I.; Carta, M.; Malpass-Evans, R.; Ferrari, M. C.; Bernardo, P.; Clarizia, G.; Jansen, J. C.; McKeown, N. B. Highly Permeable Benzotriptycene-Based Polymer of Intrinsic Microporosity. *ACS Macro Lett.* **2015**, *4* (9), 912-915.
(13) Foster, A. B.; Tamaddondar, M.; Luque-Alled, J. M.; Harrison, W. J.; Li, Z.; Gorgojo, P.; Budd, P. M. Understanding the Topology of the Polymer of Intrinsic Microporosity PIM-1: Cyclics, Tadpoles, and Network Structures and Their Impact on Membrane Performance. *Macromolecules* **2020**, *53* (2), 569-583.
(14) Mi, Y.; Stern, S. A.; Trohalaki, S. Dependence of the gas-permeability of some polyimide isomers on their intrasegmental mobility. *J. Membr. Sci.* **1993**, *77* (1), 41-48.
(15) Tanaka, K.; Kita, H.; Okamoto, K.; Nakamura, A.; Kusuki, Y. Gas Permeability and Permselectivity in Homo- and Copolyimides from 3,3',4,4'-Biphenyltetracarboxylic Dianhydride and 3,3'- and 4,4'-Diaminodiphenylsulfones. *Polym. J.* **1990**, *22* (5), 381-385.
(16) Coleman, M. R.; Koros, W. J. The transport properties of polyimide isomers containing hexafluoroisopropylidene in the diamine residue. *J. Polym. Sci., Part B: Polym. Phys.* **1994**, *32* (11), 1915-1926.
(17) Brandt, W. W. Model Calculation of the Temperature Dependence of Small Molecule Diffusion in High Polymers. *J. Phys. Chem.* **1959**, *63* (7), 1080-1084.
(18) Li, K. H.; Zhu, Z. Y.; Dong, H.; Li, Q. X.; Ji, W. H.; Li, J. X.; Cheng, B. W.; Ma, X. H. Bottom up approach to study the gas separation properties of PIM-PIs and its derived CMSMs by isomer monomers. *J. Membr. Sci.* **2021**, *635*, 119519.
(19) Zhu, Z. Y.; Zhu, J. J.; Li, J. X.; Ma, X. H. Enhanced Gas Separation Properties of Troger's Base Polymer Membranes Derived from Pure Triptycene Diamine Regioisomers. *Macromolecules* **2020**, *53* (5), 1573-1584.
(20) Hu, X. F.; Miao, J.; Pang, Y. Y.; Zhao, J. Y.; Lu, Y.; Guo, H. L.; Wang, Z.; Yan, J. L. Synthesis, microstructures, and gas separation performance of norbornyl bis-benzocyclobutene-Troger's base polymers derived from pure regioisomers. *Polym. Chem.* **2022**, *13* (19), 2842-2849.
(21) Liu, S.; Jin, Z. X.; Teo, Y. C.; Xia, Y. Efficient Synthesis of Rigid Ladder Polymers via Palladium Catalyzed Annulation. *J. Am. Chem. Soc.* **2014**, *136* (50), 17434-17437.
(22) Lai, H. W. H.; Liu, S.; Xia, Y. Norbornyl benzocyclobutene ladder polymers: conformation and microporosity. *J. Polym. Sci., Part A: Polym. Chem.* **2017**, *55* (18), 3075-3081.
(23) Lai, H. W. H.; Teo, Y. C.; Xia, Y. Functionalized Rigid Ladder Polymers from Catalytic Arene-Norbornene Annulation Polymerization. *ACS Macro Lett.* **2017**, *6* (12), 1357-1361.
(24) Lai, H. W. H.; Benedetti, F. M.; Jin, Z.; Teo, Y. C.; Wu, A. X.; De Angelis, M. G.; Smith, Z. P.; Xia, Y. Tuning the Molecular Weights, Chain Packing, and Gas-Transport Properties of CANAL Ladder Polymers by Short Alkyl Substitutions. *Macromolecules* **2019**, *52* (16), 6294-6302.
(25) Lai, H. W. H.; Benedetti, F. M.; Ahn, J. M.; Robinson, A. M.; Wang, Y. G.; Pinnau, I.; Smith, Z. P.; Xia, Y. Hydrocarbon Ladder Polymers with Ultrahigh Permselectivity for Membrane Gas Separations. *Science* **2022**, *375* (6587), 1390-1392.
(26) Struik, L. C. E. Physical aging in plastics and other glassy materials. *Polym. Eng. Sci.* **1977**, *17* (3), 165-173.
(27) Hutchinson, J. M. Physical aging of polymers. *Prog. Polym. Sci.* **1995**, *20* (4), 703-760.
(28) Swaidan, R.; Ghanem, B.; Litwiller, E.; Pinnau, I. Physical Aging, Plasticization and Their Effects on Gas Permeation in “Rigid” Polymers of Intrinsic Microporosity. *Macromolecules* **2015**, *48* (18), 6553-6561.(29) Robeson, L. M. Correlation of separation factor versus permeability for polymeric membranes. J. Membr. Sci. **1991**, *62* (2), 165-185.

SYNOPSIS TOC